

NEUROIMAGING

CSF glucose tracks regional tau progression based on Alzheimer's disease risk factors

Colleen Pappas¹ | Brandon S. Klinedinst² | Scott Le^{1,3} | Qian Wang¹ |
Brittany Larsen¹ | Kelsey McLimans⁴ | Samuel N. Lockhart⁵ | Karin Allenspach-Jorn⁶ |
Jonathan P. Mochel⁶ | Auriel A. Willette^{1,2,7,8,9} | for the Alzheimer's Disease
Neuroimaging Initiative[†]

¹ Department of Food Science and Human Nutrition, Iowa State University, Ames, Iowa, USA

² Neuroscience Graduate Program, Iowa State University, Ames, Iowa, USA

³ Interdepartmental Graduate Program, Iowa State University, Ames, Iowa, USA

⁴ Department of Nutrition and Dietetics, Viterbo University, La Crosse, Wisconsin, USA

⁵ Department of Internal Medicine, Wake Forest University, Winston-Salem, North Carolina, USA

⁶ Department of Veterinary Clinical Sciences, Iowa State University, Ames, Iowa, USA

⁷ Department of Biomedical Sciences, Iowa State University, Ames, Iowa, USA

⁸ Department of Psychology, Iowa State University, Ames, Iowa, USA

⁹ Department of Neurology, University of Iowa, Iowa City, Iowa, USA

Correspondence

Auriel A. Willette, 1109 HSNB, 706 Morrill Rd,
Ames, IA 50011-1078.

E-mail: awillett@iastate.edu

[†] Data used in preparation of this article were obtained from the Alzheimer's Disease Neuroimaging Initiative (ADNI) database (adni.loni.usc.edu). As such, the investigators within the ADNI contributed to the design and implementation of ADNI and/or provided data but did not participate in analysis or writing of this report. A complete listing of ADNI investigators can be found at: http://adni.loni.usc.edu/wp-content/uploads/how_to_apply/ADNI_Acknowledgement_List.pdf

Abstract

Introduction: Glucose hypometabolism and tau formation are key features of Alzheimer's disease (AD). Less is known about the relationship between fasting glucose and regional tau accumulation.

Methods: Cerebrospinal fluid (CSF) glucose was linearly regressed on regional tau (flortaucipir) among 169 Alzheimer's Disease Neuroimaging Initiative (ADNI3) participants. Flortaucipir uptake was examined by Braak stages and regions of interest (ROIs). Interactions were explored between CSF glucose and AD risk factors including regional amyloid beta ($A\beta$), sex, Apolipoprotein E $\epsilon 4$ ($APOE\epsilon 4$) status, AD parental family history (AD FH), and cognitive impairment (CI).

Results: Interactions found higher CSF glucose tracked less tau in ROIs or Braak stages I/II (women, $APOE \epsilon 4+$, regional $A\beta$), III/IV (AD FH+, regional $A\beta$), and V/VI (AD FH+). CI drove Braak III-VI associations.

Discussion: Among women and $APOE \epsilon 4$ carriers, higher CSF glucose tracked less early-stage tau. Higher CSF glucose may reflect compensation against tau spreading in CI, $A\beta+$, or AD FH+.

KEYWORDS

amyloid beta, apolipoprotein E, cerebrospinal fluid markers, cognitive impairment, family history of Alzheimer's disease, glucose, positron magnetic imaging, tau

This is an open access article under the terms of the [Creative Commons Attribution-NonCommercial](https://creativecommons.org/licenses/by-nc/4.0/) License, which permits use, distribution and reproduction in any medium, provided the original work is properly cited and is not used for commercial purposes.

© 2020 The Authors. *Alzheimer's & Dementia: Translational Research & Clinical Interventions* published by Wiley Periodicals LLC on behalf of Alzheimer's Association

1 | BACKGROUND

Alzheimer's disease (AD) pathology is characterized by amyloid beta ($A\beta$) accumulation and neurofibrillary tau tangles, followed by region-specific atrophy, which finally leads to the presentation of cognitive symptoms.^{1,2} In AD, tau becomes hyperphosphorylated, forms paired helical filaments, and is a consistent marker for neurodegeneration.³⁻⁵ The regional progression of tau deposition in AD has been outlined by Braak staging, beginning in the entorhinal cortex and hippocampus, then extending to cortical association areas in later AD stages.^{6,7} Braak staging has been associated with AD-related cognitive decline in aged adults, suggesting that tau deposition is also a useful proxy for the degree of cognitive impairment (CI).^{8,9} Recently, the radioligand AV-1451 (flortaucipir) has been used to quantify tau deposition *in vivo* using positron emission tomography (PET).¹⁰ Visualizing regional tau across the AD continuum provides more insight about neurodegeneration as the disease progresses. However, it is unclear what factors predict regional tau deposition and may be potential therapeutic targets, as well as how genetic and neuropathological risk factors modulate these associations.

Dysregulation of glucose production and use may be a marker of tau cleavage¹¹ and phosphorylation.¹² In addition to $A\beta$ and tau, dynamic changes in glucose metabolism occur based on disease status, fasting serum glucose levels, and region of interest (ROI).¹³⁻¹⁵ Increased tau phosphorylation also occurs during glucose deprivation in h-tau mice.¹⁶ Similarly, db/db mouse models of type II diabetes show increased tau phosphorylation in the neocortex and hippocampus.¹⁷ Thus, systemic factors related to glucose regulation may influence tau formation.

However, among individuals with CI (ie, mild cognitive impairment [MCI] due to AD and AD), greater tau deposition does not track hypometabolism in AD-sensitive ROIs.¹⁸ Critically, glucose may be a compensatory mechanism relative to central tau among at-risk individuals based on $A\beta$ status, AD parental family history (AD FH), apolipoprotein E $\epsilon 4$ (*APOE* $\epsilon 4$) status, and biological sex. These factors moderate tau deposition and links between greater metabolic dysfunction and higher CSF tau levels.¹⁹⁻²¹ This may be particularly important for $A\beta+$ status or being a woman, which are related to more regional tau in medial and inferior temporal²² and superior parietal regions.²³ Further, women who are *APOE* $\epsilon 4+$ or $A\beta+$, respectively, have greater overall tau²⁴ or more regional tau in entorhinal cortex,²³ typically the first area to show neurodegeneration in AD.

The current study used data from the Alzheimer's Disease Neuroimaging Initiative (ADNI)²⁵ to examine regional tau associations with CSF glucose levels, as an indirect index of higher non-metabolized parenchymal glucose reported in AD.²⁶ CSF glucose levels are approximately two-thirds that of plasma glucose.²⁷ We hypothesized that higher CSF glucose concentrations would predict less tau deposition, and explored if various AD risk factors such as $A\beta$ status, AD FH, *APOE* $\epsilon 4$ status, and sex modified given associations.

RESEARCH IN CONTEXT

- 1. Systematic Review:** We searched PubMed for the following key terms: cerebrospinal fluid (CSF) glucose, regional tau, Braak staging, tau phosphorylation, cognition, fluorodeoxyglucose-positron emission tomography (FDG-PET), insulin resistance, and glucose metabolism. While regional FDG and tau have been correlated, CSF levels represent both bound and unbound glucose rather than metabolized levels only.
- 2. Interpretation:** Results suggested that higher fasting CSF glucose predicted less regional tau, but only among individuals at greater risk for developing Alzheimer's disease (AD). Higher CSF glucose levels could represent a compensatory mechanism against tau deposition or a neurodegeneration biomarker.
- 3. Future Directions:** Longitudinal CSF glucose, insulin resistance, and regional tau associations would test if modulation by specific AD risk factors tracks AD-specific patterns of tau accumulation. AD risk factor modulation should also be considered when examining glucose metabolism and biomarkers of energy regulation.

2 | METHODS

2.1 | Cohort and participants

Baseline data from 169 late middle-aged to aged adults were obtained from the ADNI database (adni.loni.usc.edu). The ADNI was launched in 2003 as a public-private partnership, led by Principal Investigator Michael W. Weiner, MD. The primary goal of ADNI has been to test whether serial magnetic resonance imaging, PET, other biological markers, and clinical and neuropsychological assessment can be combined to measure the progression of MCI due to AD and early AD. For up-to-date information, see www.adni-info.org. Written informed consent was obtained from all ADNI participants at their respective ADNI sites. The ADNI protocol was approved by site-specific institutional review boards.

Participants were clinically classified by cognitive status as cognitively unimpaired (CU), MCI, or AD as described elsewhere.²⁸ Eligibility criteria for analyses included complete data for: (1) CSF glucose; (2) an 18F-AV-1451 tau PET scan; (3) age; (4) sex; (5) clinical diagnosis; and (6) AD FH. There were 175 participants with regional tau and CSF glucose data. Several participants ($n = 5$) lacked AD FH data. Additionally, we removed one outlier (>3.29 SD from the mean) for CSF glucose. This resulted in a total sample of 169 participants. A subsample had regional PET- $A\beta$ data for a corresponding visit ($n = 142$) and *APOE* genotype data ($n = 166$).

2.2 | Cerebrospinal fluid markers

CSF was obtained from lumbar puncture at baseline after at least 6 hours fasting, as described in the ADNI3 protocol (https://adni.loni.usc.edu/wp-content/uploads/2012/10/ADNI3-Procedures-Manual_v3.0_20170627.pdf). CSF glucose levels (mg/dL) were downloaded from the LOCLAB dataset.

2.3 | PET—regional tau

Regional tau deposition was measured by the PET radioligand 18F-AV-1451 (flortaucipir). As described in the ADNI PET Technical Manual (http://adni.loni.usc.edu/wp-content/uploads/2012/10/ADNI3_PET-Tech-Manual_V2.0_20161206.pdf), participants were injected with a 370 MBq ($\pm 10\%$) dose of AV-1451. After an uptake period of 75 minutes, six 5-minute scans were conducted for a total period of 30 minutes. Processed data were downloaded from the University of California Berkeley AV-1451 dataset, including mean uptake in areas constituting Braak stages I/II, III/IV, and V/VI.⁷ Standardized uptake value ratios (SUVRs) were normalized, with inferior cerebellar gray matter used as the reference region. Data were not partial volume corrected and SUVRs were averaged over both hemispheres to create bilateral ROIs.

2.4 | PET—global and regional amyloid deposition

We downloaded data for two PET tracers that were used to measure fibrillar $A\beta$ deposition in the brain via PET: florbetaben (FBB; $n = 69$) and florbetapir (AV-45; $n = 73$). Methods for collection and processing have been described previously for ADNI.^{25,29}

First, we classified participants by global amyloid deposition status (ie, $A\beta^-$ vs $A\beta^+$) based on an SUVR $> = 1.08$ ³⁰ for florbetaben and SUVR $> = 1.11$ for florbetapir.³¹ These cutoffs are specific to the ADNI sample and derived from the National Institute on Aging-Alzheimer's Association (NIA-AA) criteria for $A\beta^-$ versus $A\beta^+$.⁴ Global SUVR scores were determined by calculating mean uptake in the frontal, anterior and posterior cingulate, lateral parietal, and lateral temporal regions, using the whole cerebellum as the reference region.

Mean SUVR per bilateral ROI was also used in interactions analyses. While differences by acquisition method for the relative SUVRs in each ROI were not significant ($P_s > .05$), recent work by Klunk et al.³² has provided a method for scaling SUVRs across acquisition types and processing methods. Relative $A\beta$ deposition is expressed in Centiloid units anchored at 0 and 100, with higher numbers indicating more amyloid.³² Therefore, we converted all regional SUVRs to Centiloid units as outlined in an ADNI white paper.³³

2.5 | Neuropsychological testing

ADNI uses an extensive battery of tests to examine cognitive functioning with a particular emphasis on domains relevant to AD. A

full description is available at <http://adni.loni.usc.edu>. All subjects underwent clinical and neuropsychological assessment at the time of scan acquisition. Neuropsychological assessments included the Clinical Dementia Rating sum of boxes (CDR-SB), mini-Mental State Examination (MMSE), Rey Auditory Verbal Learning Test, and AD Assessment Scheduled Cognition-11 (ADAS-Cog11).

2.6 | Dichotomization of clinical impairment

Due to the small sample sizes of MCI and AD participants, a dichotomized categorical variable was created by comparing participants with CI ($n = 47$) to CU ($n = 122$).

2.7 | AD parental family history

Participants were classified as having or not having a family history of AD. Family history was defined by self-report as one or both parents having had AD.

2.8 | APOE $\epsilon 4$ genotype

APOE haplotype was determined using blood samples and has been previously described.³⁴ APOE status was dichotomized as $\epsilon 4$ non-carriers (no $\epsilon 4$ alleles) versus $\epsilon 4$ carriers (one or two $\epsilon 4$ alleles).

2.9 | Statistical analyses

To test sample characteristic differences between diagnostic groups, analysis of variance and Fisher's exact tests were performed. Pearson correlations tested the association between each predictor variable and tau deposition for each ROI. In the case in which a specific ROI was not normally distributed, Spearman correlations were used.

Multiple linear regression was then done to examine the relationship between CSF glucose levels and regional tau deposition. We initially examined mean signal for Braak ROIs comprising stage I/II, stage III/IV, or stage V/VI. Subsequently, we examined a priori selected ROIs from stage I/II or stage III/IV, due to the sample largely being composed of CU individuals who would typically not have the presence of tau in stage V/VI ROIs (see Table S1 in supporting information for details). Age (in years) and sex (male vs female) were used as covariates in the statistical model. Exploratory analyses using the version 3.1 PROCESS macro for SAS³⁵ also tested modulation interactions between CSF glucose and sex (male vs female), APOE $\epsilon 4$ status (APOE $\epsilon 4+$ vs $\epsilon 4-$), global $A\beta$ status ($A\beta^-$ vs $A\beta^+$), Centiloid-based amyloid in the same ROI as regional tau SUVR, AD FH (AD FH+ vs AD FH-), and cognitive impairment status (CU vs CI). To contain type 1 error, these follow-up interactions were considered significant at $P < .10$.^{36,37}

The Johnson-Neyman technique³⁸ was then used via the PROCESS macro to interpret interactions for continuous moderator variables (ie,

TABLE 1 Characteristics of participants by cognitive status

Characteristic	Cognitively unimpaired (n = 122)	Mild cognitive impairment (n = 38)	Alzheimer's disease (n = 9)
Age, mean (SD), y	71.17 (6.04)	72.41 (8.04)	74.36 (11.43)
Female, %	68.03	42.11	33.33
Education, mean (SD), y	16.92 (2.26)*	15.68 (2.56)	16.22 (2.77)
MMSE Score, mean (SD)	29.22 (0.99)**†	28.13 (2.11)†	21.56 (3.21)
A β +, %	33.01	48.39	87.50
AD Parental Family History, %	36.07	31.58	66.67
APOE ϵ 4 Carrier, %	32.50	36.84	50.00
CSF Glucose, mean (SD), mg/dL	58.55 (6.51)	57.95 (6.94)	61.56 (10.20)

Abbreviations: A β , amyloid beta; APOE, apolipoprotein E; AV-45; florbetapir; CSF, cerebrospinal fluid; FBB, florbetaben; MCI, mild cognitive impairment; MMSE, Mini-Mental State Examination; PET, positron emission tomography; SD, standard deviation.

Notes: Values from AV-45 and FBB PET scans were used to categorized A β + vs A β - participants; these data were only available for a subset of individuals (n = 142) who were cognitively unimpaired (n = 103), MCI (n = 31), or AD (n = 8). Likewise, APOE genotype was only for a subset of participants (n = 166) who were cognitively unimpaired (n = 120), MCI (n = 38), or AD (n = 8).

*P < .05 compared to the MCI group; **P < .001 compared to the MCI group; †P < .001 compared to the AD group

regional A β deposition). Briefly, this technique provides a significant point estimate for the moderator and percentage of the sample above and below this estimate, rather than testing effects at a predetermined value such as ± 1 standard deviation of the mean.³⁵

Analyses were completed using SAS software version 9.4 (Cary, North Carolina). Alpha was set at .05 with stringent correction for type 1 error using several methods. For main effects analyses with multiple outcomes, a multivariate analysis of covariance (MANCOVA) omnibus test was conducted. A significant omnibus difference allowed follow-up ROI-specific models at a family-wise error rate of .05.³⁹ If the omnibus MANCOVA was not significant, family-wise error was contained using Holm-Bonferroni methods as described.¹³

3 | RESULTS

3.1 | Participant characteristics

Participant characteristics by diagnostic status are displayed in Table 1. The overall sample was approximately 71.6 years old, had over 16 years of education, and the majority were female (60.4%). The mean CSF glucose level was 58.6 mg/dL, which is within the normal range of 45–80 mg/dL.⁴⁰ Approximately one third of the sample (36.7%) had AD FH, with similar prevalence observed for A β + (39.4%) or APOE ϵ 4+ (34.3%) status.

Age and CSF glucose levels were similar between diagnostic groups. Participants with MCI had fewer years of education as compared to CU participants (P < .05); no other differences were present. Poorer performance across the AD spectrum was found for MMSE scores. Additionally, the distribution of females and A β + individuals by cognitive status differed (Ps < .05), but were similar for AD FH+ or APOE ϵ 4+ status.

3.2 | Correlations

Bivariate correlations between demographics, CSF glucose, and Braak staging classifications are reported in Table S2 in supporting information. In general, greater regional tau deposition was associated with being CI or A β +. Across all participants, higher CSF glucose was related to less regional tau deposition only in the caudal anterior cingulate gyrus.

3.3 | Multiple linear regression—main effects

Across all participants, CSF glucose was not associated with tau deposition when examining the collective Braak I/II, III/IV, or V/VI staging regions (Ps > .05). However, as with correlations, CSF glucose levels were inversely related to tau deposition in the caudal anterior cingulate gyrus (F(3,165) = 3.11, P = .028, R² = .054, unstandardized beta [β] = -.0029, standard error [SE] = 0.001, P = .024). This result was no longer significant after type 1 error correction.

3.4 | Multiple linear regression—interaction/moderation analyses

Significant CSF glucose by moderator interactions for Braak stages or a priori determined ROIs is summarized in Table 2, where Figure 1 A-C depicts coverage in neocortical regions. Briefly, there were patterns of association that reflected early to later Braak stages, which were respectively seen with separate interactions for sex, APOE ϵ 4+, regional A β +, and AD FH+ specific to the ROI being tested. Figure 2 illustrates a matrix of cells summarizing significant interactions for

TABLE 2 Interactions with CSF glucose for regional tau deposition

Region of interest	F-value	R ²	p-value	Interaction β	SE	p-value	95% CI
Sex							
Hippocampus	2.44	.056	.049	-.006	.003	.072	-.013, .001
Apolipoprotein E ϵ4 status							
Hippocampus	3.30	.094	.007	-.008	.004	.091	-.016, .001
Amygdala	5.82	.154	<.001	-.014	.006	.013	-.025, -.003
Global Aβ							
Parahippocampal	7.35	.213	<.001	-.005	.003	.095	-.012, .001
Regional Aβ							
Entorhinal	6.21	.186	<.001	-.0003	.0001	.016	-.0005, -.0001
Hippocampus	7.41	.214	<.001	-.0002	.0001	.080	-.0004, .0000
Parahippocampal	11.15	.288	<.001	-.0001	.0001	.018	-.0003, -.0000
Lingual	9.90	.267	<.001	-.0001	.0000	.054	-.0002, -.0000
Fusiform	18.60	.406	<.001	-.0002	.0001	.005	-.0003, -.0000
Inferior temporal	16.43	.377	<.001	-.0001	.0001	.014	-.0002, -.0000
Amygdala	9.44	.258	<.001	-.0002	.0001	.039	-.0004, -.0000
Parental family history of Alzheimer's disease							
Braak III/IV	2.60	.074	.027	-.009	.004	.017	-.017, -.002
Braak V/VI	2.54	.072	.030	-.005	.003	.048	-.011, -.000
Parahippocampal	2.47	.070	.035	-.006	.003	.066	-.013, .000
Lingual	3.87	.106	.002	-.012	.003	<.001	-.019, -.006
Fusiform	3.68	.101	.004	-.016	.005	.002	-.026, -.006
Isthmus of cingulate	2.58	.073	.028	-.010	.004	.011	-.018, -.002
Cognitive status							
Caudal anterior cingulate	3.35	.093	.007	-.006	.003	.025	-.011, -.001
Posterior cingulate	3.47	.096	.005	-.006	.003	.080	-.012, .001

Abbreviations: A β , amyloid beta; CI, confidence interval; CSF, cerebrospinal fluid; SE, standard error.

Note: All ROIs listed are $P < .10$ for interactions, and were significant by group at follow-up ($P < .05$).

Braak stages or ROIs across all participants ("gray"). A description of the results by each moderator follows.

3.5 | Moderation by sex

A significant CSF glucose by sex interaction was found for the hippocampus (Table 2), such that higher CSF glucose was linked to less regional tau in women but not men (see Table 3).

3.6 | Moderation by APOE ϵ 4 status

APOE ϵ 4 status by CSF glucose interactions were observed for the hippocampus and the amygdala (Table 2). Higher CSF glucose levels were associated with less regional tau deposition for APOE ϵ 4+ but not APOE ϵ 4- (see Table 3).

3.7 | Moderation by global A β and ROI regional A β

For global A β status, higher CSF glucose was related to less tau deposition among A β + but not A β - for the parahippocampal gyrus (Tables 2 and 3).

Interactions were then tested between CSF glucose and regional A β (as a continuous measure) derived from the same given ROI as regional tau. For ROIs in Braak Stage I/II and III/IV (Table 2), higher CSF glucose significantly corresponded to less tau deposition only when A β in the same region reached a data-driven cut-point using the Johnson-Neyman technique. These ROIs included medial and inferior temporal regions.

For the entorhinal cortex, amygdala, and lingual gyrus, higher A β moderated the higher CSF glucose and less regional tau relationship in a small portion of the total sample (<20%), which may be due to most participants being CU. Given this sample size imbalance, and a lack of robustness for regression estimates with $n < 30$, follow-up analyses are not further reported.

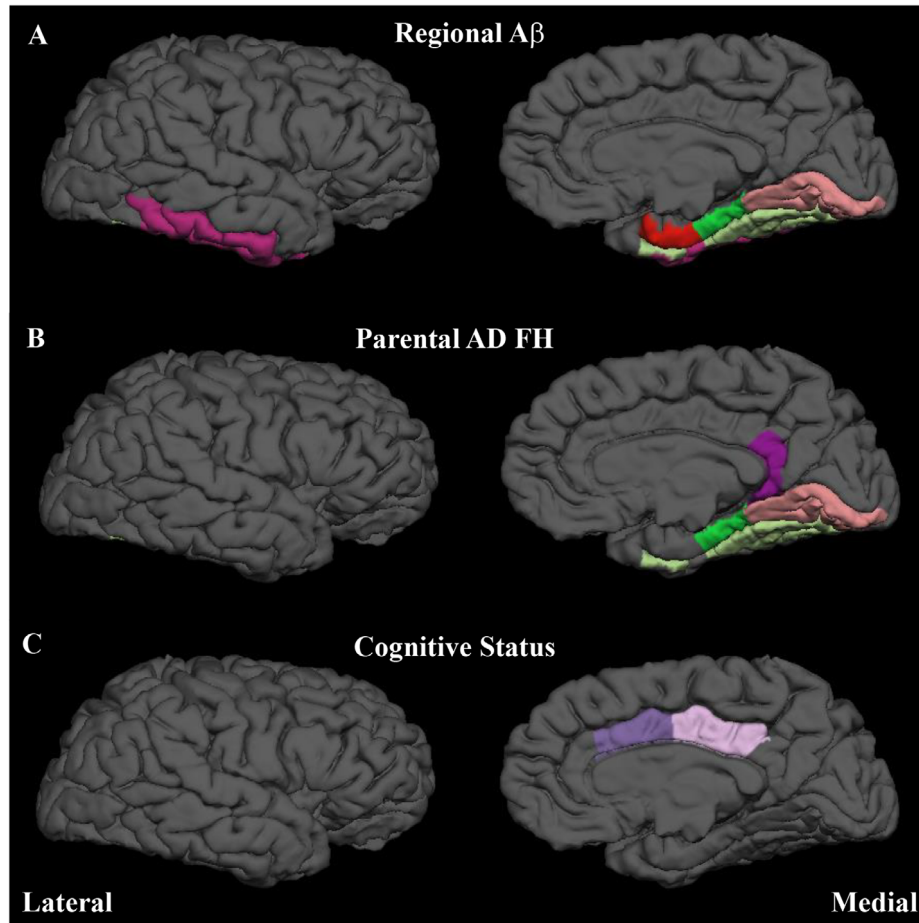


FIGURE 1 Differences in regional tau staging associations based on cerebrospinal fluid (CSF) glucose and moderators. Regions of interest are shown for interactions between CSF glucose and (A) regional amyloid-beta ($A\beta$) deposition, (B) parental Alzheimer's disease family history (AD FH), and (C) cognitive status groups (unimpaired vs impaired, ie, mild cognitive impairment [MCI] + AD). For regional $A\beta$ deposition, significant regions of interest (ROIs) included parahippocampal gyrus (green), entorhinal cortex (red), hippocampus (not pictured), amygdala (not pictured), lingual (pink), fusiform (mint), and inferior temporal gyri (magenta). For AD FH, significant ROIs included the parahippocampal gyrus (green), lingual (pink) and fusiform (mint) gyri, and the isthmus of the cingulate (dark purple). For cognitive status, significant ROIs included caudal anterior (lilac) and posterior cingulate (purple). Allocortical or subcortical ROIs are not shown for sex (hippocampus) and apolipoprotein E (hippocampus, amygdala)

For the hippocampus, a Centiloid value of 29.27 or higher was the critical point where regional $A\beta$ moderated the glucose-tau relationship, which was observed in 32% of the sample. Similar results were observed for the parahippocampus at a Centiloid value of 13.34 or higher (25% of sample), the fusiform gyrus at a Centiloid value of 32.75 or higher (28% of sample), and the inferior temporal gyrus at a Centiloid value of 41.45 or higher (25% of sample; Figure 3 and Figure S1 in supporting information).

3.8 | Moderation by AD FH

Higher CSF glucose levels were associated with less regional tau among AD FH+ but not FH- for Braak III/IV and Braak V/VI stages, as well as specific ROIs including the parahippocampal gyrus, lingual gyrus, fusiform gyrus, and isthmus of the posterior cingulate (Tables 2 and 3).

3.9 | Moderation by cognitive status

Among CI but not CU participants, higher CSF glucose levels were associated with less tau deposition in the caudal anterior cingulate and posterior cingulate gyri (Tables 2 and 3).

3.10 | Exploratory CSF glucose analyses by cognitive status group

On an exploratory basis, we stratified participants by cognitive status (CU vs CI) and re-ran all moderation analyses. We acknowledge that these interaction analyses are underpowered for the CI participants. Results are reported in Tables S3–S5 in supporting information and displayed as a matrix of cells in Figure 2, showing where only CU (“black”) or CI (“red”) groups evinced an association between CSF glucose and tau.

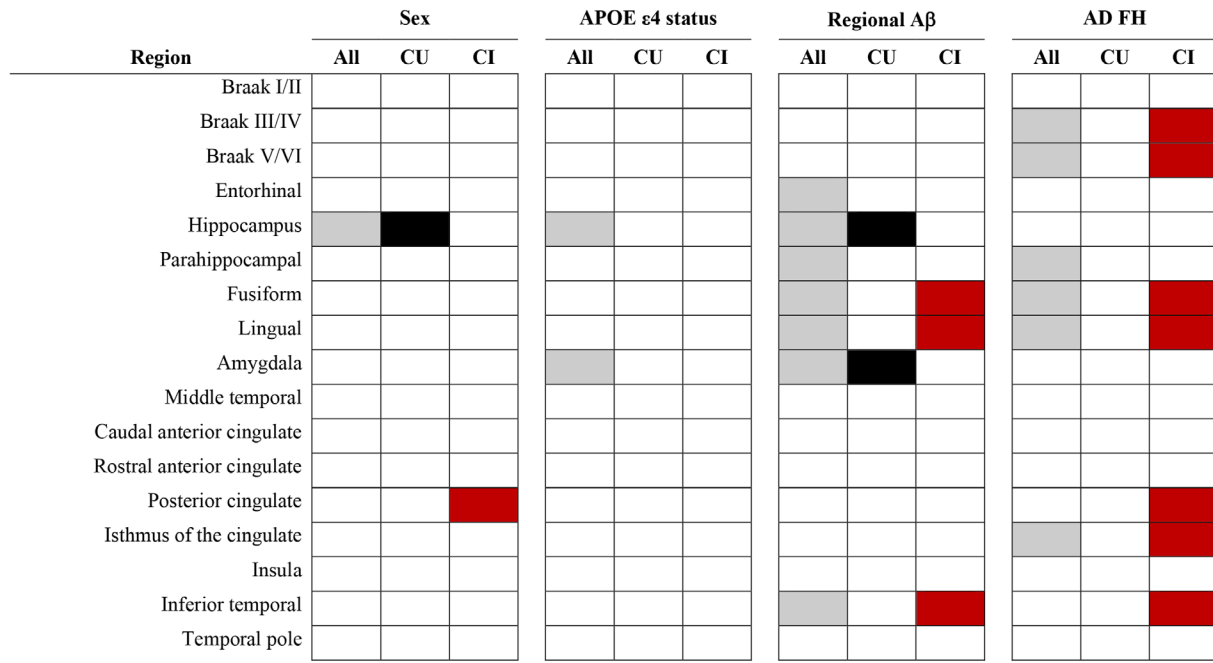


FIGURE 2 Regional tau associations based on cerebrospinal fluid (CSF) glucose, moderators, and cognitive status. Region of interest (ROI) associations with CSF glucose for the entire sample (gray), only cognitively unimpaired participants (CU; black), or only cognitively impaired (CI; red) participants. Only significant ROIs are included ($P < .10$ for interactions; $P < .05$ for follow-up analyses)

TABLE 3 Estimates by group for CSF glucose-moderator interactions

Region of Interest	β	SE	β	SE
Sex				
Men (n = 67) Women (n = 102)				
Hippocampus	-.000	.002	-.006	.003*
Apolipoprotein E ϵ4 status				
ϵ 4-(n = 109) ϵ 4+(n = 57)				
Hippocampus	-.002	.002	-.009	.004*
Amygdala	.002	.002	-.012	.005*
Global Aβ status				
A β -(n = 86) A β +(n = 56)				
Parahippocampal	-.0003	.002	-.0056	.002*
Parental family history of AD				
FH-(n = 107) FH+(n = 62)				
Braak III/IV	.002	.002	-.008	.003*
Braak V/VI	.000	.002	-.005	.002*
Parahippocampal	.000	.002	-.006	.003*
Lingual	.003	.002	-.010	.003**
Fusiform	.003	.003	-.013	.004*
Isthmus of cingulate	.002	.002	-.009	.003*
Cognitive status				
CU (n = 122) CI (n = 47)				
Caudal anterior cingulate	-.001	.002	-.007	.002*
Posterior cingulate	-.000	.002	-.006	.003*

Abbreviations: A β +, global amyloid positive; A β -, global amyloid negative; AD, Alzheimer's disease; CSF, cerebrospinal fluid; CI, cognitively impaired; CU, cognitively unimpaired; FH, family history.

* $P < .05$; ** $P < .001$.

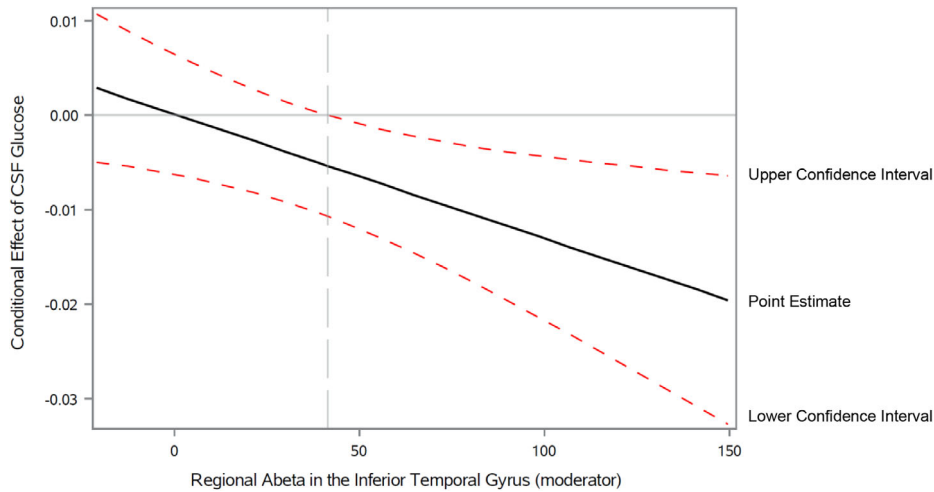


FIGURE 3 Cerebrospinal fluid (CSF) glucose by regional amyloid beta ($A\beta$) interaction for the inferior temporal gyrus using the Johnson-Neyman technique. Regional $A\beta$ in the inferior temporal gyrus and moderation of the relationship between more CSF glucose and less hippocampal tau deposition. Using the Johnson-Neyman technique, higher CSF glucose levels were associated with less tau deposition for participants with inferior temporal gyrus $A\beta$ centiloid values at or above 41.45 (indicated by the vertical gray dotted line). This encompassed approximately 25% of the sample. The black line represents the overall estimate and the red dotted lines represent the 95% confidence interval

For sex moderation, higher CSF glucose and less tau were found among CU participants in the hippocampus and among CI participants in the posterior cingulate (Table S3). For regional $A\beta$ moderation, associations of higher glucose, and less tau were seen among CU participants for ROIs comprising Braak stage I/II and III/IV and among CI participants for ROIs comprising Braak stages III/IV (Table S4). For AD FH, CI but not CU participants showed significant higher glucose and less tau relationships in Braak stage III/IV and V/VI ROIs (Table S5). No $APOE \epsilon 4$ status or global $A\beta$ interactions were observed.

4 | DISCUSSION

The current study examined the relationship between CSF glucose levels and regional PET tau deposition across the AD spectrum. Overall, higher CSF glucose was related to less regional tau deposition almost exclusively among individuals with CI or at greater AD risk due to sex, $APOE \epsilon 4$ status, $A\beta$ load, and AD FH. Specifically, higher CSF glucose tracked less tau in ROIs or Braak stages I/II (female sex, $APOE \epsilon 4+$, $A\beta+$), III/IV (AD FH+, $A\beta+$), and V/VI (AD FH+). Exploratory analyses further suggested that CI appeared to drive Braak III-VI associations, although caution is warranted due to small sample size.

While higher glucose levels have been associated with poorer cognitive abilities⁴¹ and less brain volume,⁴² we did not find a detrimental effect between elevated CSF glucose and tau. Higher glucose levels may instead be an initial compensatory mechanism to protect against disease pathophysiology. AD is marked by brain hypometabolism, but hypermetabolism can occur in MCI.⁴³ Insulin resistance, which often reflects increased glucose production, also predicted hypermetabolism in the medial temporal lobe among MCI individuals that converted to AD.¹³ Our results similarly suggest that higher CSF glucose levels in

aged adults with AD risk factors may be a marker of or mechanism for less tau pathology. Further, tau is innately involved with brain and peripheral insulin signaling, potentially through a positive feedback loop.⁴⁴ Glucose metabolism is also upregulated in microglia, particularly in relation to amyloid clearance.⁴⁵ Alternatively, higher CSF glucose levels may simply be part of the initial neurodegenerative processes related to early stage tau phosphorylation. Since higher CSF glucose was linked to less tau in this study, lower glucose might lead to greater tau deposition and disease progression. However, recent work shows that AD versus CU participants have higher brain glucose levels,²⁶ suggesting that higher CSF glucose in AD may be a compensatory mechanism for tau-related neurodegeneration.

Regardless, higher CSF glucose and less tau followed an interesting moderation pattern for Braak stages I/II (female, $APOE \epsilon 4+$, higher regional $A\beta$), stages III/IV (higher regional $A\beta$, CI), and stages III/VI (AD FH+). As central glucose metabolism reflects $A\beta$ deposition,¹⁹ region-specific tau accumulation may first be driven by risk factors modifying regional $A\beta$ and later glycolytic impairments due to AD FH+. For sex and $APOE \epsilon 4$, CSF glucose interactions were observed in the hippocampus or hippocampus and amygdala, respectively. Both women and $APOE \epsilon 4$ carriers showed a stronger relationship between more medial temporal tau and $A\beta$ levels.^{23,46} Higher CSF total tau and p-tau are also seen only in $APOE \epsilon 4$ carriers with MCI,⁴⁷ corresponding to what those changes would be in the temporal lobe.

In concert, regional $A\beta$ modified CSF glucose associations through these initial Braak stage I/II areas and stages III/IV. Using the Johnson-Neyman technique to establish $A\beta$ cutoffs where CSF glucose-tau associations became significant, we found that regional $A\beta$ was progressively higher for later versus earlier Braak stages. Among CU participants with global $A\beta+$, hypometabolism is associated with more tau in the medial temporal lobe.¹⁹ Tau also accumulates over time⁴⁸ in Braak stages I-IV ROIs similar to those regions observed in the current study

(eg, entorhinal cortex, fusiform gyrus, inferior temporal gyrus). As $A\beta$ drives hypometabolism in medial temporal lobe-specific regions with more tau,¹⁹ CSF glucose may reflect the relative degree to which parenchymal tissue uses glucose and maintains physiological cellular processes.

Finally, AD FH+ only modified CSF glucose-tau relationships in later Braak stages. There is a paucity of data regarding the relationship between AD FH and regional tau, although elevated CSF tau/ $A\beta$ levels have been previously reported.²¹ Maternal FH has also been associated with glucose hypometabolism in temporal and cingulate areas, akin to where we found CSF glucose and tau relationships.⁴⁹ Therefore, AD FH may come into play later in tau progression.

Strengths and limitations of the study should be noted. While many reports have examined the association between fluorodeoxyglucose (FDG)-PET and regional tau, we are the first to evaluate a CSF marker of available glucose. Our work adds to a growing body of research implicating glucose regulation in AD pathogenesis. We accounted for moderating effects of AD-related risk factors, and if participants were CU or CI. However, the sample consisted mostly of individuals classified as CU, which may impact the interpretation of our results for those already displaying cognitive symptoms. Given the cross-sectional data, we could not test the directionality of the observed glucose-tau relationship. Careful interpretation is also needed for the hippocampus, as there is the potential for non-specific binding.⁵⁰ Further, at the time of this study, ADNI3 did not include data on biological assays beyond a complete blood count. Serum glucose measures were not available for comparison. However, an upregulation of CSF metabolic markers (eg, lactate dehydrogenase B-chain, pyruvate kinase) has been implicated with AD,⁴⁵ which lends credence to our CSF glucose results. We also could not test underlying biological mechanisms linking CSF glucose to regional tau. Future studies should examine CSF or serum-based markers that are related to mitochondrial function and metabolism by use of proteomics in relation to tau progression.

In conclusion, CSF glucose levels were only related to regional tau deposition in at-risk groups in the present study. APOE ϵ 4 status and sex impacted associations for earlier stage Braak stages and ROIs, while regional $A\beta$, cognitive status, and AD FH influenced mid- to late-stage Braak ROIs. The risk factors studied herein may be synergistically acting with glucose levels in response to tau development, or may be a proxy of neurodegeneration. While we cannot confirm these hypotheses with cross-sectional data, results add to a growing body of research highlighting the impact of metabolic factors and also suggest that markers of circulating brain glucose may modify relationships with AD tau pathology.

ACKNOWLEDGMENTS

This study was funded by Iowa State University, NIH R00 AG047282, and AARGD-17-529552. No funding provider had any role in the conception, collection, execution, or publication of this work. Data collection and sharing for this project was funded by the Alzheimer's Disease Neuroimaging Initiative (ADNI; National Institutes of Health Grant U01 AG024904) and DOD ADNI (Department of Defense award number W81XWH-12-2-0012). ADNI is funded by the National

Institute on Aging, the National Institute of Biomedical Imaging and Bioengineering, and through generous contributions from the following: AbbVie; Alzheimer's Association; Alzheimer's Drug Discovery Foundation; Araclon Biotech; BioClinica, Inc.; Biogen; Bristol-Myers Squibb Company; CereSpir, Inc.; Cogstate; Eisai Inc.; Elan Pharmaceuticals, Inc.; Eli Lilly and Company; EuroImmun; F. Hoffmann-La Roche Ltd and its affiliated company Genentech, Inc.; Fujirebio; GE Healthcare; IXICO Ltd.; Janssen Alzheimer Immunotherapy Research & Development, LLC; Johnson & Johnson Pharmaceutical Research & Development LLC; Lumosity; Lundbeck; Merck & Co., Inc.; Meso Scale Diagnostics, LLC; NeuroRx Research; Neurotrack Technologies; Novartis Pharmaceuticals Corporation; Pfizer Inc.; Piramal Imaging; Servier; Takeda Pharmaceutical Company; and Transition Therapeutics. The Canadian Institutes of Health Research is providing funds to support ADNI clinical sites in Canada. Private sector contributions are facilitated by the Foundation for the National Institutes of Health (www.fnih.org). The grantee organization is the Northern California Institute for Research and Education, and the study is coordinated by the Alzheimer's Therapeutic Research Institute at the University of Southern California. ADNI data are disseminated by the Laboratory for Neuro Imaging at the University of Southern California.

REFERENCES

1. Jack CR, Jr., Knopman DS, Jagust WJ, et al. Tracking pathophysiological processes in Alzheimer's disease: an updated hypothetical model of dynamic biomarkers. *Lancet Neurol.* 2013;12:207-216.
2. Jack CR, Jr., Knopman DS, Jagust WJ, et al. Hypothetical model of dynamic biomarkers of the Alzheimer's pathological cascade. *Lancet Neurol.* 2010;9:119-128.
3. Iqbal K, Liu F, Gong CX, Grundke-Iqbal I. Tau in Alzheimer disease and related tauopathies. *Curr Alzheimer Res.* 2010;7:656-664.
4. Jack CR, Jr, Bennett DA, Blennow K, et al. NIA-AA Research Framework: toward a biological definition of Alzheimer's disease. *Alzheimers Dement.* 2018;14:535-562.
5. Santa-Maria I, Varghese M, Ksiazek-Reding H, Dzhun A, Wang J, Pasinetti GM. Paired helical filaments from Alzheimer disease brain induce intracellular accumulation of Tau protein in aggresomes. *J Biol Chem.* 2012;287:20522-20533.
6. Braak H, Alafuzoff I, Arzberger T, Kretschmar H, Del Tredici K. Staging of Alzheimer disease-associated neurofibrillary pathology using paraffin sections and immunocytochemistry. *Acta Neuropathol.* 2006;112:389-404.
7. Braak H, Braak E. Neuropathological staging of Alzheimer-related changes. *Acta Neuropathol.* 1991;82:239-259.
8. Grober E, Dickson D, Sliwinski MJ, et al. Memory and mental status correlates of modified Braak staging. *Neurobiol Aging.* 1999;20:573-579.
9. Brier MR, Gordon B, Friedrichsen K, et al. Tau and Abeta imaging, CSF measures, and cognition in Alzheimer's disease. *Sci Transl Med.* 2016;8:338ra66.
10. Schöll M, Lockhart SN, Schonhaut DR, et al. PET imaging of tau deposition in the aging human brain. *Neuron.* 2016;89:971-982.
11. Kim B, Backus C, Oh S, Feldman EL. Hyperglycemia-induced tau cleavage in vitro and in vivo: a possible link between diabetes and Alzheimer's disease. *J Alzheimers Dis.* 2013;34:727-739.
12. Wu J, Zhou SL, Pi LH, et al. High glucose induces formation of tau hyperphosphorylation via Cav-1-mTOR pathway: a potential molecular mechanism for diabetes-induced cognitive dysfunction. *Oncotarget.* 2017;8:40843-40856.

13. Willette AA, Modanlo N, Kapogiannis D, Alzheimer's Disease Neuroimaging I. Insulin resistance predicts medial temporal hypermetabolism in mild cognitive impairment conversion to Alzheimer disease. *Diabetes*. 2015;64:1933-1940.
14. Edison P, Archer HA, Hinz R, et al. Amyloid, hypometabolism, and cognition in Alzheimer disease: an [11C]PIB and [18F]FDG PET study. *Neurology*. 2007;68:501-508.
15. Gray KR, Wolz R, Heckemann RA, Aljabar P, Hammers A, Rueckert D. Multi-region analysis of longitudinal FDG-PET for the classification of Alzheimer's disease. *Neuroimage*. 2012;60:221-229.
16. Lauretti E, Li JG, Di Meco A, Pratico D. Glucose deficit triggers tau pathology and synaptic dysfunction in a tauopathy mouse model. *Transl Psychiatry*. 2017;7:e1020.
17. Kim B, Backus C, Oh S, Hayes JM, Feldman EL. Increased tau phosphorylation and cleavage in mouse models of type 1 and type 2 diabetes. *Endocrinology*. 2009;150:5294-5301.
18. Chiotis K, Saint-Aubert L, Rodriguez-Vieitez E, et al. Longitudinal changes of tau PET imaging in relation to hypometabolism in prodromal and Alzheimer's disease dementia. *Mol Psychiatry*. 2018;23:1666-1673.
19. Adams JN, Lockhart SN, Li L, Jagust WJ. Relationships between tau and glucose metabolism reflect Alzheimer's disease pathology in cognitively normal older adults. *Cereb Cortex*. 2019;29:1997-2009.
20. Starks EJ, O'Grady JP, Hoscheidt SM, et al. Insulin resistance is associated with higher cerebrospinal fluid tau levels in asymptomatic APOE ϵ 4 Carriers. *J Alzheimers Dis*. 2015;46:525-533.
21. Honea RA, Vidoni ED, Swerdlow RH, Burns JM. Maternal family history is associated with Alzheimer's disease biomarkers. *J Alzheimers Dis*. 2012;31:659-668.
22. Das SR, Xie L, Wisse LEM, et al. Longitudinal and cross-sectional structural magnetic resonance imaging correlates of AV-1451 uptake. *Neurobiol Aging*. 2018;66:49-58.
23. Buckley RF, Mormino EC, Rabin JS, et al. Sex differences in the association of global amyloid and regional tau deposition measured by positron emission tomography in clinically normal older adults. *JAMA Neurol*. 2019;76:542-551.
24. Hohman TJ, Dumitrescu L, Barnes LL, et al. Sex-specific association of apolipoprotein E with cerebrospinal fluid levels of tau. *JAMA Neurol*. 2018;75:989-998.
25. Weiner MW, Veitch DP, Aisen PS, et al. The Alzheimer's Disease Neuroimaging Initiative 3: continued innovation for clinical trial improvement. *Alzheimers Dement*. 2017;13:561-571.
26. Mullins R, Reiter D, Kapogiannis D. Magnetic resonance spectroscopy reveals abnormalities of glucose metabolism in the Alzheimer's brain. *Ann Clin Transl Neurol*. 2018;5:262-272.
27. Leen WG, Willemsen MA, Wevers RA, Verbeek MM. Cerebrospinal fluid glucose and lactate: age-specific reference values and implications for clinical practice. *PLoS One*. 2012;7:e42745-e.
28. Petersen RC, Aisen PS, Beckett LA, et al. Alzheimer's Disease Neuroimaging Initiative (ADNI): clinical characterization. *Neurology*. 2010;74:201-209.
29. Jagust WJ, Landau SM, Koeppel RA, et al. The Alzheimer's Disease Neuroimaging Initiative 2 PET Core: 2015. *Alzheimer's & dementia: the journal of the Alzheimer's Association*. 2015;11:757-771.
30. Landau S, Jagust W, Florabetaben processing and positivity threshold derivation. 2018.
31. Landau SM, Mintun MA, Joshi AD, et al. Amyloid deposition, hypometabolism, and longitudinal cognitive decline. *Ann Neurol*. 2012;72:578-586.
32. Klunk WE, Koeppel RA, Price JC, et al. The Centiloid Project: standardizing quantitative amyloid plaque estimation by PET. *Alzheimer's & Dementia*. 2015;11:1-15.
33. Kolibash SA, Minhas D, Lopresti BJ, Centiloid level-2 analysis of [18F]florabetaben (FBB) and [18F]florbetapir (FBP) PET image data using the ADNI pipeline. 2018.
34. Saykin AJ, Shen L, Yao X, et al. Genetic studies of quantitative MCI and AD phenotypes in ADNI: progress, opportunities, and plans. *Alzheimer's & Dementia*. 2015;11:792-814.
35. Hayes AF. *Introduction to Mediation, Moderation, and Conditional Process Analysis: A Regression-Based Approach*. 2nd ed. New York: The Guilford Press; 2018.
36. Geijselaers SLC, Aalten P, Ramakers IHGB, et al. Association of cerebrospinal fluid (CSF) insulin with cognitive performance and CSF biomarkers of Alzheimer's disease. *J Alzheimers Dis*. 2018;61:309-320.
37. Selvin S. *Statistical Analysis of Epidemiologic Data*. New York: Oxford University Press; 1996.
38. Johnson PO, Neyman J. Tests of certain linear hypotheses and their application to some educational problems. *Statistical Research Memoirs*. 1936;1.
39. Hummel TJ, Sligo JR. Empirical comparison of univariate and multivariate analysis of variance procedures. *Psychol Bull*. 1971;76:49-57.
40. Roos K. *Principles of Neurologic Infectious Diseases*. New York: McGraw-Hill, Medical Publication Division; 2005.
41. Anstey KJ, Sargent-Cox K, Eramudugolla R, Magliano DJ, Shaw JE. Association of cognitive function with glucose tolerance and trajectories of glucose tolerance over 12 years in the AusDiab study. *Alzheimers Res Ther*. 2015;7:48.
42. Cherbuin N, Sachdev P, Anstey KJ. Higher normal fasting plasma glucose is associated with hippocampal atrophy: the PATH Study. *Neurology*. 2012;79:1019-1026.
43. Ashraf A, Fan Z, Brooks DJ, Edison P. Cortical hypermetabolism in MCI subjects: a compensatory mechanism. *Eur J Nucl Med Mol Imaging*. 2015;42:447-458.
44. Marciniak E, Leboucher A, Caron E, et al. Tau deletion promotes brain insulin resistance. *J Exp Med*. 2017;214:2257-2269.
45. Johnson ECB, Dammer EB, Duong DM, et al. Large-scale proteomic analysis of Alzheimer's disease brain and cerebrospinal fluid reveals early changes in energy metabolism associated with microglia and astrocyte activation. *Nat Med*. 2020.
46. Corder EH, Ghebremedhin E, Taylor MG, Thal DR, Ohm TG, Braak H. The biphasic relationship between regional brain senile plaque and neurofibrillary tangle distributions: modification by age, sex, and APOE polymorphism. *Ann N Y Acad Sci*. 2004;1019:24-28.
47. Liu Y, Tan L, Wang HF, et al. Multiple effect of APOE genotype on clinical and neuroimaging biomarkers across Alzheimer's disease spectrum. *Mol Neurobiol*. 2016;53:4539-4547.
48. Jack CR, Jr., Wiste HJ, Schwarz CG, et al. Longitudinal tau PET in ageing and Alzheimer's disease. *Brain*. 2018;141:1517-1528.
49. Mosconi L, Brys M, Switalski R, et al. Maternal family history of Alzheimer's disease predisposes to reduced brain glucose metabolism. *Proc Natl Acad Sci U S A*. 2007;104:19067-19072.
50. Baker SL, Maass A, Jagust WJ. Considerations and code for partial volume correcting [(18)F]-AV-1451 tau PET data. *Data Brief*. 2017;15:648-657.

SUPPORTING INFORMATION

Additional supporting information may be found online in the Supporting Information section at the end of the article.

How to cite this article: Pappas C, Klinedinst BS, Le S, et al. CSF glucose tracks regional tau progression based on Alzheimer's disease risk factors. *Alzheimer's Dement*. 2020;6:e12080. <https://doi.org/10.1002/trc2.12080>